# Temperature-dependent fine structure splitting in InGaN quantum dots

Tong Wang,[1,a)] Tim J. Puchtler,[1,a)] Tongtong Zhu,[2] John C. Jarman,[2] Claudius C. Kocher[1], Rachel A. Oliver,[2] and Robert A. Taylor[1]

[1]*Department of Physics, University of Oxford, Parks Road, Oxford, OX1 3PU, UK*

[2]*Department of Materials Science and Metallurgy, University of Cambridge, 27 Charles Babbage Road, Cambridge CB3 0FS, UK*

We report the experimental observation of temperature-dependent fine structure splitting in semiconductor quantum dots using a non-polar (11-20) *a*-plane InGaN system, up to the on-chip Peltier cooling threshold of 200 K. At 5 K, a statistical average splitting of 443 ± 132 μeV has been found based on 81 quantum dots. The degree of fine structure splitting stays relatively constant for temperatures less than 100 K, and only increases above that temperature. At 200 K, we find that the fine structure splitting ranges between 2 ~ 12 meV, which is an order of magnitude higher than that at low temperatures. Our investigations also show that phonon interactions at high temperatures might have a correlation with the degree of exchange interactions. The large fine structure splitting at 200 K makes it easier to isolate the individual components of the polarized emission spectrally, increasing the effective degree of polarization for potential on-chip applications of polarized single-photon sources.

Polarized single-photon emitters[1] are essential elements in various quantum information applications. Engineering the polarization state of single photons enables the use of qubits in optical quantum computing[2] and implementation of polarization-based quantum key distribution protocols.[3,4] Many systems, such as single atoms,[5] molecules[6], diamond nitrogen vacancy centers,[7] and silicon carbide defects,[8] have demonstrated the emission of single photons. However, for practical integration into electrically driven solid-state systems, semiconductor quantum dots[9] (QDs) have been at the forefront of single-photon research. Much progress has been made with arsenide-based QD systems,[10–12] which are capable of generating ultrapure and near indistinguishable photons. However, their lack of intrinsic polarization properties and ability to operate at elevated temperatures offers limited prospect for realistic and efficient on-chip applications. In contrast to arsenide systems which operate in the infrared range, InGaN provides single photon sources in the blue spectral region, enabling efficient free space transmission and detection. Furthermore, the large and tunable band offsets in nitrides offer much stronger quantum confinement, allowing operations at temperatures significantly higher than cryogenic conditions. A few nitride-based systems

[a)] Electronic mails: tong.wang@physics.ox.ac.uk; tim.puchtler@physics.ox.ac.uk.

have demonstrated single-photon emission above 200 K, a temperature reachable by Peltier cooling, thus promising in-principle single-photon applications in on-chip temperature conditions.[13–18] No work has been done to date to address the fine structure splitting (FSS) of a QD system at high temperatures, which is both a topic of fundamental interest and a yet unknown factor that could affect the on-chip operability of polarized single-photon emission, e.g. the ability to generate polarization-entangled photon pairs.

In general, for the same material and composition, QD shape anisotropy causes polarized emission in a direction determined by the specific geometry of the nanostructure, with a strong and weak emission component polarized orthogonal to each other. The exchange interaction between electrons and holes results in two distinct exciton ground state transitions, each associated with one of these polarization states. The energy difference between these two states is called the FSS. Size differences, shape anisotropies, and material content fluctuations of QDs affect the spatial part of the electron and hole wavefunctions,[19,20] and thus the strength of exchange, resulting in differences in the FSS of each QD. This is especially so in self-assembled systems.

For nitride QDs, the effect of anisotropy is found to be especially pronounced. Hence, the commonly used polar (0001) nitride QDs generally exhibit polarized emission with a random axis and degree of polarization.[21,22] In the *a*-plane (11-20) nitride system, polarized emission is caused by asymmetric strain in the growth plane giving rise to a lowering of the wurtzite symmetry to orthorhombic, an effect much stronger than that of anisotropy. Recent development of non-polar (11-20) *a*-plane InGaN QDs have demonstrated a statistically high average polarization degree of 0.90, with a deterministic polarization axis along the crystal *m*-direction.[23] The reduction of the undesired quantum confined Stark effect also produces much faster radiative exciton recombination rate,[24] thus reducing the probability of non-radiative recombination at elevated temperatures. This increased quantum efficiency allows *a*-plane QDs to reach temperatures in the Peltier-cooled regime, and makes investigations of temperature-dependent FSS possible.

In this work, we report experimentally measured FSS values of *a*-plane InGaN QDs at 5 K with statistical significance, and compare these to literature results obtained in other nitride systems. More importantly, we investigate the temperature evolution of the FSS up to 200 K, also with statistical significance, and propose possible physical reasons for this evolution.

The *a*-plane InGaN QD samples were fabricated using the modified droplet epitaxy method[25,26] in a 6 × 2 in. Thomas Swan close-coupled showerhead reactor on *r*-plane sapphire substrates. The precursors gases used were trimethylgallium, trimethylindium, and ammonia. The epitaxial layer overgrowth (ELOG) technique was used to achieve a reduced defect

density in the pseudo-substrate. At 695°C and 300 Torr, a ~ 10 ML InGaN epilayer was grown and annealed in $N_2$ atmosphere for 30 s. The subsequent decomposition of the quantum well (QW) and formation of metallic clusters is followed by the growth of a 10 nm GaN capping layer at the same temperature, during which QD formation occurs. A final 10 nm of GaN is grown at 1050°C using $H_2$ as the carrier gas. The as-grown wafers were then processed by etching to produce nanopillars (d ~180 nm) in order to limit the number of QDs under examination and increase photon extraction efficiencies.

The optical properties of the QDs were assessed by time-integrated micro-photoluminescence (μ-PL). The QD sample was placed in an AttoDRY800 close-cycle cryogenic system, which maintains a stable temperature of 5 K, and is capable of regulating temperature changes up to ambient conditions. A Ti:Sapphire laser operating at a repetition rate of 76 MHz provides pulsed excitation of 1 ps duration at 800 nm. The choice of two-photon excitation allows QDs to have higher relative absorption cross-sections than the underlying InGaN QW,[27] thereby facilitating optical characterization of the QDs. The excitation pulses were coupled into a single-mode fiber and then directed to a 100× objective with 0.5 N.A., producing a ~ 1 μm diameter spot for sample excitation. The PL from the sample was collected by the same objective, and passed on to a half-wave plate and a polarizer for polarization-resolved investigations and to maintain a constant input polarization for the spectrometer. The placement of the sample was such that the emission polarized along the *m*(*c*)-direction corresponded to 0°(90°) of the polarizer and 0°(-45°) of the half-wave plate. The PL then entered the 100 μm slit of a Shamrock 500i half-meter spectrograph, and was dispersed by a 1200l/mm grating. A Peltier-cooled Andor iDus 420 charge-couple device is used for low-noise detection and imaging with a spectral resolution of ~ 38 pm.

Ideally, for any QD with a polarization degree less than unity, the FSS should be measurable. However, the linewidths of InGaN QDs (~ 0.5 to 3 meV) are comparable to their typical FSS (< 1 meV),[28] making their identification very challenging. Furthermore, in our *a*-plane system, very weak emission from the *c*-direction polarized fine structure component makes the study of QD emission energy in this direction difficult and imprecise. Experimentally, FSS could only be resolved accurately for QDs with polarization degrees lower than ~ 0.80.

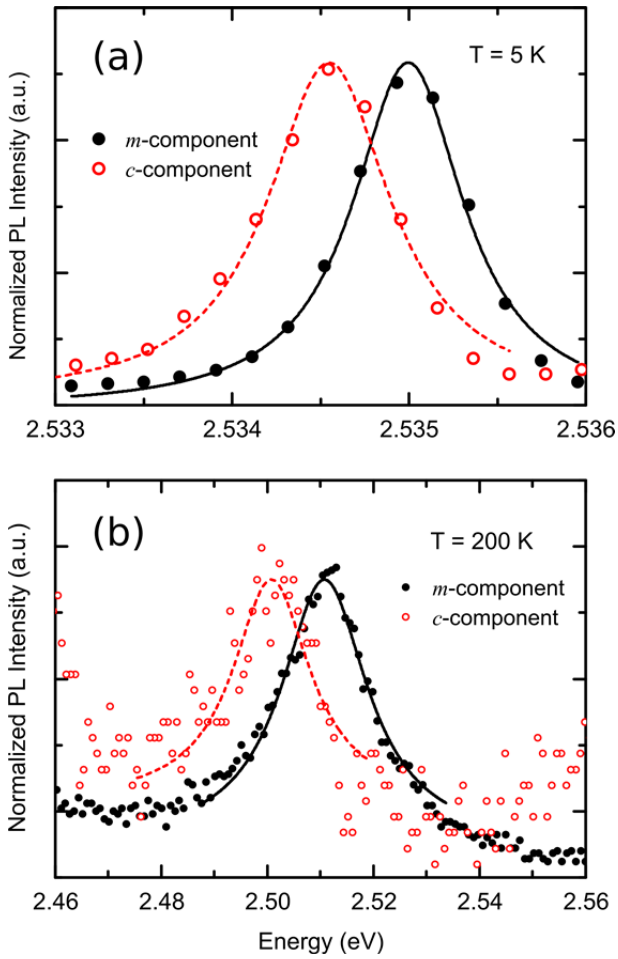


FIG. 1. μ-PL spectra of the QD emission polarized along *m*- and *c*-direction of the sample respectively at (a) 5 K and (b) 200 K. The intensities of the weaker *c*-components have been normalized by factors of (a) 8.34 and (b) 5.97.

A QD with a polarization degree of ~ 0.79 was chosen for this study. The polarization-resolved PL spectra of the QD at 5 K are shown in Fig. 1(a). The peak intensity of the PL component parallel to the *c*-axis of the sample has been normalized to that parallel to the *m*-axis. Since the linewidth is much larger than the Fourier-limited Lorentzian linewidth, emission data of both components have been fitted to Gaussian profiles to account for broadening caused by the presence of fluctuating electric fields resulting from local charge trapping, i.e. spectral diffusion. The broadened linewidth of ~ 1 meV is a result of the fast-timescale spectral diffusion, caused by mobile carriers in the quantum well matrix, as opposed to discrete spectral jumps produced by slower diffusion, arising from carrier trapping in defects near the QDs.[29] The peak emission energies of the *m*- and *c*-component obtained from the fitting are 2535.00 ± 0.01 meV and 2534.55 ± 0.02 meV respectively. We

attribute this energy difference between the two peaks mainly to the FSS. With the definition of FSS = $|E_m - E_c|$, where $E_m$ and $E_c$ are peak energies of the *m*- and *c*-component respectively, the FSS of this QD at 5 K can then be calculated to be 450 ± 22 μeV, which agrees with previously published polar and non-polar InGaN FSS values.[28,30,31]

We then increased the temperature of the same QD, and performed the same polarization-resolved PL measurements at each temperature step. At 200 K, the emission intensity has decreased drastically, and the linewidth broadened significantly, both contributing to more difficulty in the measurement of emission energies, especially for the *c*-component. Nonetheless, at this temperature, we can distinctly observe the disappearance of one peak and the appearance of a different peak located in a different spectral position, as we rotate the polarizer. This is indicative of a much higher FSS value. The $E_m$ and $E_c$ at 200 K obtained from the fitting in Fig. 1(b) are 2510.7 ± 0.2 meV and 2500.7 ± 0.6 meV respectively, yielding a FSS of 10.0 ± 0.6 meV, which is an order of magnitude higher than that at 5 K. Although the degree of linear polarization decreases slightly to ~ 0.71, the much larger FSS makes it possible to select the *m*-component spectrally, with only a small contribution from the *c*-component at the same emission energy, thereby allowing a higher effective degree of polarization to be achieved in the context of the overall system.

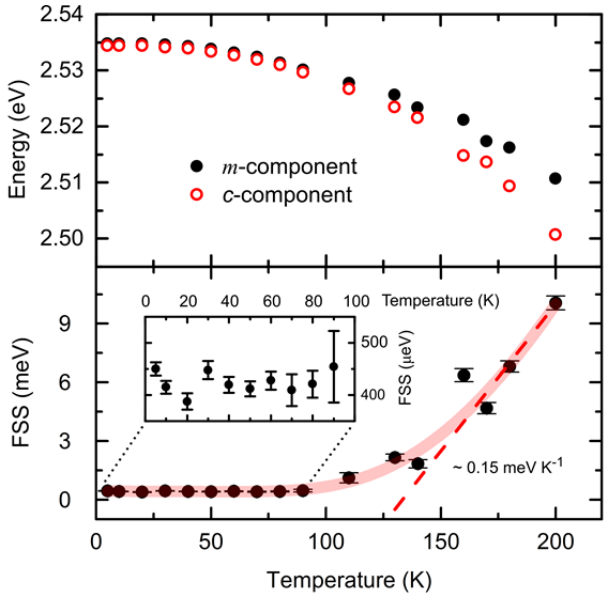


FIG. 2. Temperature dependent variations of the FSS from 5 to 200 K, arising from different temperature evolutions of the two cross-polarized components. The solid curve and dashed line are phenomenological fittings of the FSS data. The dashed line has a gradient of ~ 0.15 meV $K^{-1}$.

The temperature evolution of the FSS for the studied QD is shown in Fig. 2. Additionally, the variation of brightness and linewidth with temperature has also been analyzed and presented in the Supplementary Material (see Fig. S1). It is worth noting that the FSS value stayed relatively constant up to T ~ 100 K, and only started increasing at higher temperatures at a quasilinear rate of approximately 0.15 meV $K^{-1}$ for this particular QD. The rate of increase is slightly different for different QDs, but the FSS only starts to increase at round 100 K (see 5 other QDs in Fig. S2 in the Supplementary Material). The top of Fig. 2 also shows that for this particular QD, although both $E_m$ and $E_c$ exhibit Varshni-like decrease due to the shrinking of semiconductor bandgap at higher temperatures, $E_c$ decreases faster than $E_m$ above 100 K. The error of measurement becomes greater as T increases, due to both a reduction in brightness and greater spectral diffusion. Nonetheless, the separation of the two peaks in the spectra at T > 100 K can be measured distinctly, and hence should not be simply an effect caused by spectral diffusion. Another possible explanation could be the increased degree of exciton-phonon interaction at higher temperatures. Recent studies in AlN indicate that such an effect not only causes shifts in the exciton binding energy, but also affects the degree of exchange interaction.[32] Therefore, it is not impossible that the increase of phonon coupling, commensurate with the broadening of linewidth observed in Fig. 1(b) and Fig. S1, could have resulted in a greater FSS. Additionally, although the FSS itself increased by a factor of 60, the polarization degree only decreased by 10%. In order to fully comprehend the origin of these effects, rigorous theoretical work on configuration interaction *and* higher excited states of the exciton transition *with* consideration of phonon coupling would be required, which is well beyond the scope of this letter.

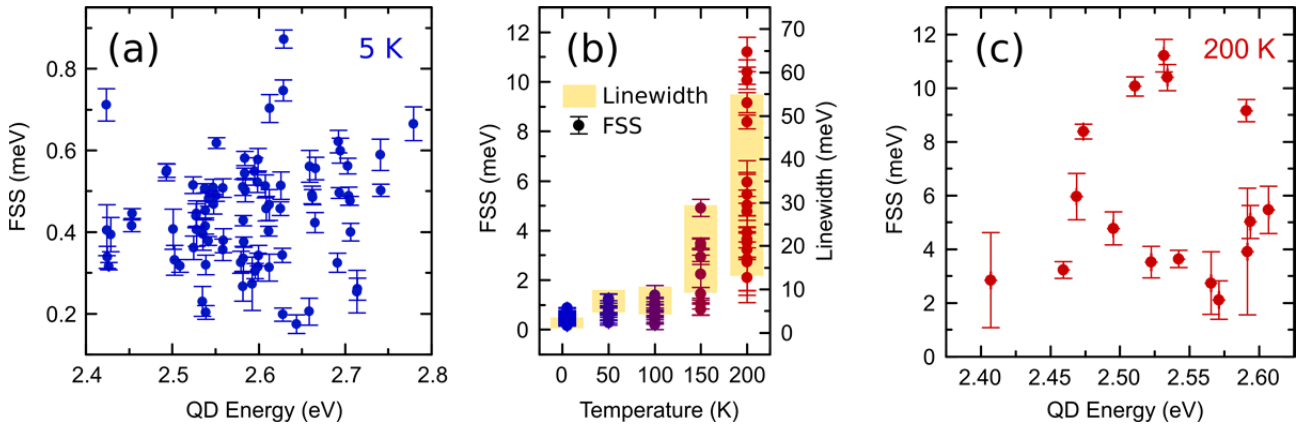


FIG. 3. (a) FSS of 81 *a*-plane InGaN QDs at arbitrary emission energies at 5 K. (b) A comparison of the 81 QDs with 10 different QDs at 50, 100 and 150 K, and 16 QDs at 200 K. A rise in average FSS occurs after 100 K. Also shown are the

ranges of linewidth of the studied QDs at each temperature step. The correlation between linewidth and FSS suggests that phonons might be affecting the extent of exchange interaction. (c) FSS of the 16 QDs plotted against emission energy at 200 K. The values obtained are an order of magnitude greater than those at 5 K.

In order to achieve statistical significance for the FSS of *a*-plane InGaN QDs at both low and high temperatures, we investigated 81 QDs with polarization degrees less than 0.8 at 5 K. The FSS data shown in Fig. 3(a) are between 100 and 900 μeV. A histogram of their distribution is included in the Supplementary Material (see Fig. S3(a)), with a calculated mean of 443 μeV and standard deviation of 132 μeV. As mentioned earlier, the self-assembled nature of the QDs will inevitably cause significant size differences, shape anisotropies, and local indium content variations, which will affect the spatial component of the exchange interaction and thus FSS, contributing to the large spread of these values. The mean FSS is about an order of magnitude larger than that in typical arsenide QDs.[33] Moreover, unlike arsenide systems, no correlations with QD energy were found.[34,35] Previous configuration interaction calculations in arsenide QDs reveal that a small QD size and higher exciton recombination energy would lead to a smaller FSS, which might not be true in nitrides where the band structures are very different. In our non-polar *a*-plane InGaN system, the lack of any observable correlation could also be due to the fact that emission wavelength is determined by many different, potentially conflicting, factors. For example the compositional variation between QDs, as well as differences in size and shape, can all alter energy levels. Hence whereas InAs QDs maintain a constant composition and vary only in size, allowing a trend between wavelength and FSS to be observed, our InGaN QDs also vary in composition, obscuring a trend which might otherwise be seen. Again, rigorous configuration interaction studies accounting for these differences based on the nitride material would need to be undertaken in order to understand the splitting properly. Nonetheless, these values are in agreement with low temperature PL and EL measurements in polar *c*-plane and non-polar *a*-plane QD systems in the available nitride literature.[28,30,31]

At higher temperatures, it starts to become harder to identify QDs exhibiting both sufficiently bright emission and low enough degrees of linear polarization. Hence, a set of 10 different QDs each at 50, 100 and 150 K, and 16 QDs at 200 K are included in this statistical investigation, as shown in Fig. 3(b). With increasing temperature, the average and range of FSS are similar at $T < 100$ K, but increase significantly at beyond 100 K. This is in agreement with our results in Fig. 1(b), 2, and S2, thereby providing statistical evidence for temperature-dependent FSS. Furthermore, as the homogeneous broadening of linewidth is partially caused by the interaction of phonons, we also included the corresponding range of linewidths measured

for the QDs at each temperature step (yellow rectangles) in Fig. 3(b). The average linewidth has a similar trend to that of FSS, implying that there could indeed be a correlation between phonons and exchange interactions in our system. As discussed earlier, fast-timescale spectral diffusion also leads to broadening of the linewidth. Since the extent of spectral diffusion might increase with temperature,[13,36] it is also important to ascertain whether the FSS increase is related to phonon scattering or spectral diffusion. For this investigation, we studied if a relationship exists between spectral diffusion and FSS at 5 K, a temperature at which the spectral diffusion dominates over phonon-assisted process. According to the data presented in Fig. S3(b) in the Supplementary Material, there is no observable correlation between linewidth and FSS at 5 K, indicating that phonon scattering is more likely to be the responsible process for the observation of FSS temperature dependence.

The FSS values of the 16 QDs studied at 200 K are shown in Fig. 3(c). All results are in the range of 2 ~ 12 meV, which are indeed an order of magnitude greater than at 5 K, in agreement with the individual QDs studied in Fig. 1, 2, and S2. Again, no discernible correlation between FSS and QD emission energy can be observed at 200 K. However, it is interesting to note that the emission energy of bright *a*-plane InGaN QDs with low degrees of polarization, which are still operating at 200 K, are mostly between 2.4 and 2.6 eV, comparing to the range of 2.4 ~ 2.8 eV in the 5 K case. This is expected, as lower emission energies are usually caused by higher indium contents, assuming similar QD size and geometry. The resultant larger band offsets and thus stronger confinement allowed these QDs to operate at higher temperatures than others. The spread of the high temperature FSS values could again be attributed to smaller variations in QD indium content, size, and shape.

In summary, we have investigated the temperature dependence of the FSS in *a*-plane InGaN QDs. An average FSS value of 443 ± 132 μeV remains relatively constant between 5 to 100 K, but starts increasing at higher temperatures until reaching 2 ~ 12 meV at 200 K. While the physical geometry, dimension, and material composition could affect the extent of the splitting, stronger phonon interactions at higher temperatures are likely to be the cause of temperature-dependent FSS. The order of magnitude greater FSS at 200 K in *a*-plane InGaN QDs makes it easier to spectrally select individual polarized components, thus resulting in higher effective polarization degrees, a feature useful for the future development of on-chip applications of polarized single-photon sources.

## SUPPLEMENTARY MATERIAL

See supplementary material for temperature evolution of brightness and linewidth of the studied single QD in Fig. 1 and 2, the temperature evolution of FSS of 5 other QDs, and additional statistical data.

## ACKNOWLEDGEMENT

This research was supported by the Engineering and Physical Sciences Research Council (EPSRC) U.K. (Grant No. EP/M012379/1 and EP/M011682/1) T.W. is grateful for the award of a National Science Scholarship (NSS) as PhD funding by the Singapore Agency for Science, Technology and Research (A*STAR). C.C.K. is grateful for the support provided by a Clarendon Scholarship and a Mary Frances and Philip Wagley Graduate Scholarship. R.A.O. is grateful to the Royal Academy of Engineering and the Leverhulme Trust for a Senior Research Fellowship.

## Note

All data presented in Fig. 1–3 are available free of charge at the DOI: 10.5287/bodleian:QRgg1nyJg

## References

[1] B. Lounis and M. Orrit, Reports Prog. Phys. **68**, 1129 (2005).

[2] D. Loss and D. P. DiVincenzo, Phys. Rev. A **57**, 120 (1998).

[3] C. H. Bennett and G. Brassard, in *Proc. IEEE Int. Conf. Comput. Syst. Signal Process.* (1984), pp. 175–179.

[4] C. Kurtsiefer, P. Zarda, M. Halder, H. Weinfurter, P. M. Gorman, P. R. Tapster, and J. G. Rarity, Nature **419**, 450 (2002).

[5] H. J. Kimble, M. Dagenais, and L. Mandel, Phys. Rev. Lett. **39**, 691 (1977).

[6] B. Lounis and W. E. Moerner, Nature **407**, 491 (2000).

[7] N. Mizuochi, T. Makino, H. Kato, D. Takeuchi, M. Ogura, H. Okushi, M. Nothaft, P. Neumann, A. Gali, F. Jelezko, J. Wrachtrup, and S. Yamasaki, Nat. Photonics **6**, 299 (2012).

[8] S. Castelletto, B. C. Johnson, V. Ivády, N. Stavrias, T. Umeda, A. Gali, and T. Ohshima, Nat. Mater. **13**, 151 (2013).

[9] S. Buckley, K. Rivoire, and J. Vučković, Reports Prog. Phys. **75**, 126503 (2012).

[10] J. Claudon, J. Bleuse, N. S. Malik, M. Bazin, P. Jaffrennou, N. Gregersen, C. Sauvan, P. Lalanne, and J.-M. Gérard, Nat. Photonics **4**, 174 (2010).

[11] Y.-M. He, Y. He, Y.-J. Wei, D. Wu, M. Atatüre, C. Schneider, S. Höfling, M. Kamp, C.-Y. Lu, and J.-W. Pan, Nat. Nanotechnol. **8**, 213 (2013).

[12] N. Somaschi, V. Giesz, L. De Santis, J. C. Loredo, M. P. Almeida, G. Hornecker, S. L. Portalupi, T. Grange, C. Anton, J.

Demory, C. Gomez, I. Sagnes, N. D. L. Kimura, A. Lemaitre, A. Auffeves, A. G. White, L. Lanco, and P. Senellart, Nat. Photonics **10**, 340 (2016).

[13] T. Wang, T. J. Puchtler, T. Zhu, J. C. Jarman, L. P. Nuttall, R. A. Oliver, and R. A. Taylor, Nanoscale **9**, 9421 (2017).

[14] S. Deshpande, T. Frost, A. Hazari, and P. Bhattacharya, Appl. Phys. Lett. **105**, 141109 (2014).

[15] S. Deshpande, A. Das, and P. Bhattacharya, Appl. Phys. Lett. **102**, 161114 (2013).

[16] M. J. Holmes, S. Kako, K. Choi, M. Arita, and Y. Arakawa, ACS Photonics **3**, 543 (2016).

[17] P. Bhattacharya, S. Deshpande, T. Frost, and A. Hazari, Proc. SPIE **9382**, 938207 (2015).

[18] S. Kako, C. Santori, K. Hoshino, S. Götzinger, Y. Yamamoto, and Y. Arakawa, Nat. Mater. **5**, 887 (2006).

[19] S. K. Patra, O. Marquardt, and S. Schulz, Opt. Quantum Electron. **48**, 151 (2016).

[20] S. K. Patra and S. Schulz, J. Phys. D: Appl. Phys. **50**, 025108 (2017).

[21] S. Amloy, K. F. Karlsson, and P. O. Holtz, arXiv: arxiv.org/abs/1311.5731v1 (2013).

[22] R. Bardoux, T. Guillet, B. Gil, P. Lefebvre, T. Bretagnon, T. Taliercio, S. Rousset, and F. Semond, Phys. Rev. B **77**, 235315 (2008).

[23] T. Wang, T. J. Puchtler, S. K. Patra, T. Zhu, M. Ali, T. J. Badcock, T. Ding, R. A. Oliver, S. Schulz, and R. A. Taylor, Nanophotonics, DOI: 10.1515/nanoph-2017-0027 (2017).

[24] S. K. Patra, T. Wang, T. J. Puchtler, T. Zhu, R. A. Oliver, R. A. Taylor, and S. Schulz, Phys. Status Solidi B, DOI: 10.1002/pssb.201600675 (2017).

[25] T. Zhu, F. Oehler, B. P. L. Reid, R. M. Emery, R. A. Taylor, M. J. Kappers, and R. A. Oliver, Appl. Phys. Lett. **102**, 251905 (2013).

[26] T. Wang, T. J. Puchtler, T. Zhu, J. C. Jarman, R. A. Oliver, and R. A. Taylor, Phys. Status Solidi B, DOI: 10.1002/ pssb. 201600724 (2017).

[27] A. F. Jarjour, A. M. Green, T. J. Parker, R. A. Taylor, R. A. Oliver, G. Andrew D. Briggs, M. J. Kappers, C. J. Humphreys, R. W. Martin, and I. M. Watson, Phys. E **32**, 119 (2006).

[28] S. Amloy, Y. T. Chen, K. F. Karlsson, K. H. Chen, H. C. Hsu, C. L. Hsiao, L. C. Chen, and P. O. Holtz, Phys. Rev. B **83**, 201307 (2011).

[29] B. P. L. Reid, T. Zhu, T. J. Puchtler, L. J. Fletcher, C. C. S. Chan, R. A. Oliver, and R. A. Taylor, Jpn. J. Appl. Phys. **52**, 08JE01 (2013).

[30] B. P. L. Reid, C. C. Kocher, T. Zhu, F. Oehler, C. C. S. Chan, R. A. Oliver, and R. A. Taylor, Appl. Phys. Lett. **106**, 171108 (2015).

[31] L. Zhang, C.-H. Teng, P.-C. Ku, and H. Deng, Phys. Rev. B **93**, 085301 (2016).

[32] R. Ishii, M. Funato, and Y. Kawakami, Jpn. J. Appl. Phys. **53**, 091001 (2014).

[33] S. Seidl, B. D. Gerardot, P. A. Dalgarno, K. Kowalik, A. W. Holleitner, P. M. Petroff, K. Karrai, and R. J. Warburton, Phys. E **40**, 2153 (2008).

[34] R. Seguin, A. Schliwa, S. Rodt, K. Potschke, U. W. Pohl, and D. Bimberg, Phys. Rev. Lett. **95**, 257402 (2005).

[35] R. J. Young, R. M. Stevenson, A. J. Shields, P. Atkinson, K. Cooper, D. A. Ritchie, K. M. Groom, A. I. Tartakovskii, and M. S. Skolnick, Phys. Rev. B **72**, 113305 (2005).

[36] T. J. Puchtler, T. Wang, C. X. Ren, F. Tang, R. A. Oliver, R. A. Taylor, and T. Zhu, Nano Lett. **16**, 7779 (2016).

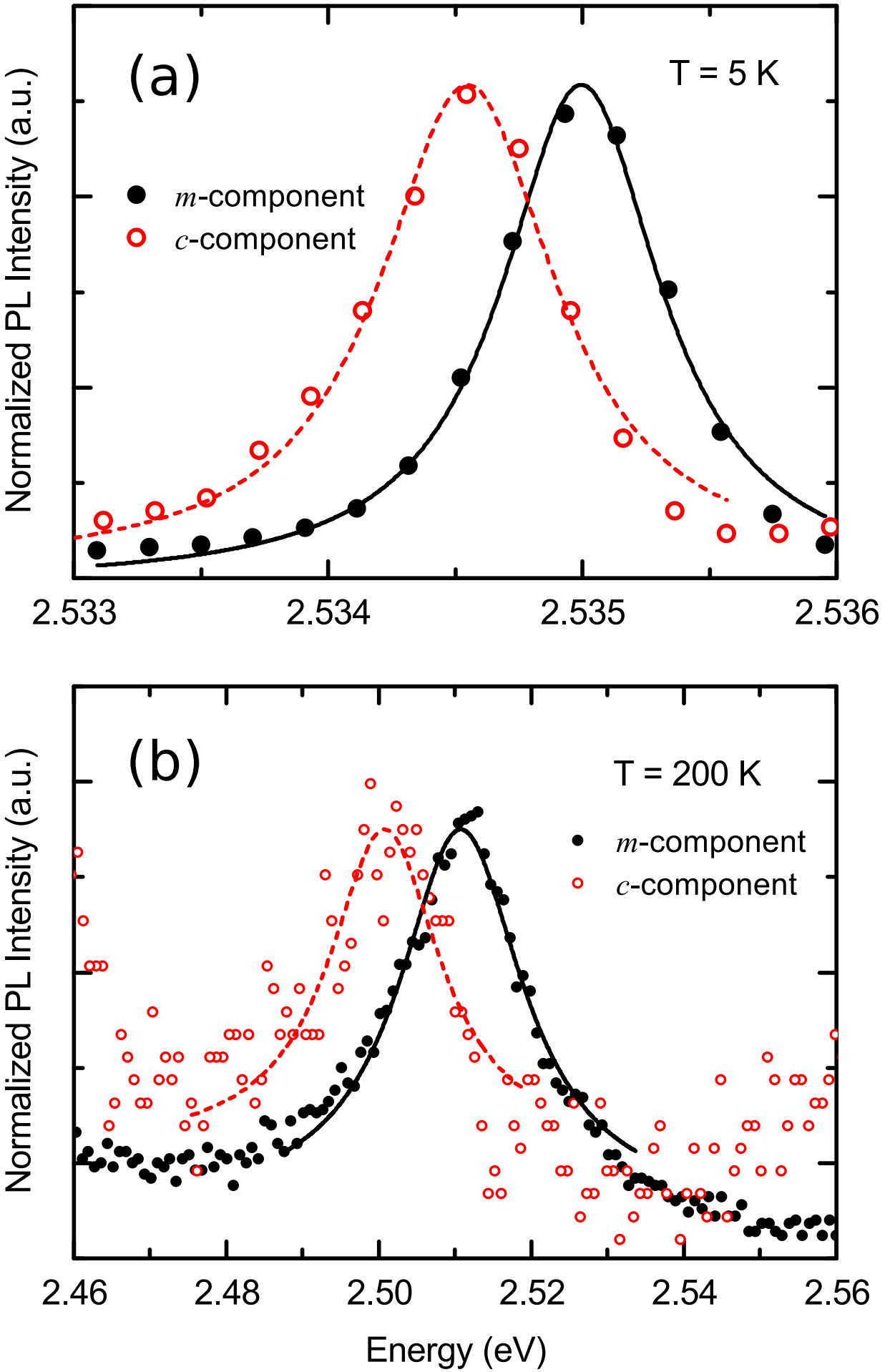
(a)
T = 5 K
m-component
c-component
Normalized PL Intensity (a.u.)
2.533
2.534
2.535
2.536
(b)
T = 200 K
m-component
c-component
Normalized PL Intensity (a.u.)
2.46
2.48
2.50
2.52
2.54
2.56
Energy (eV)

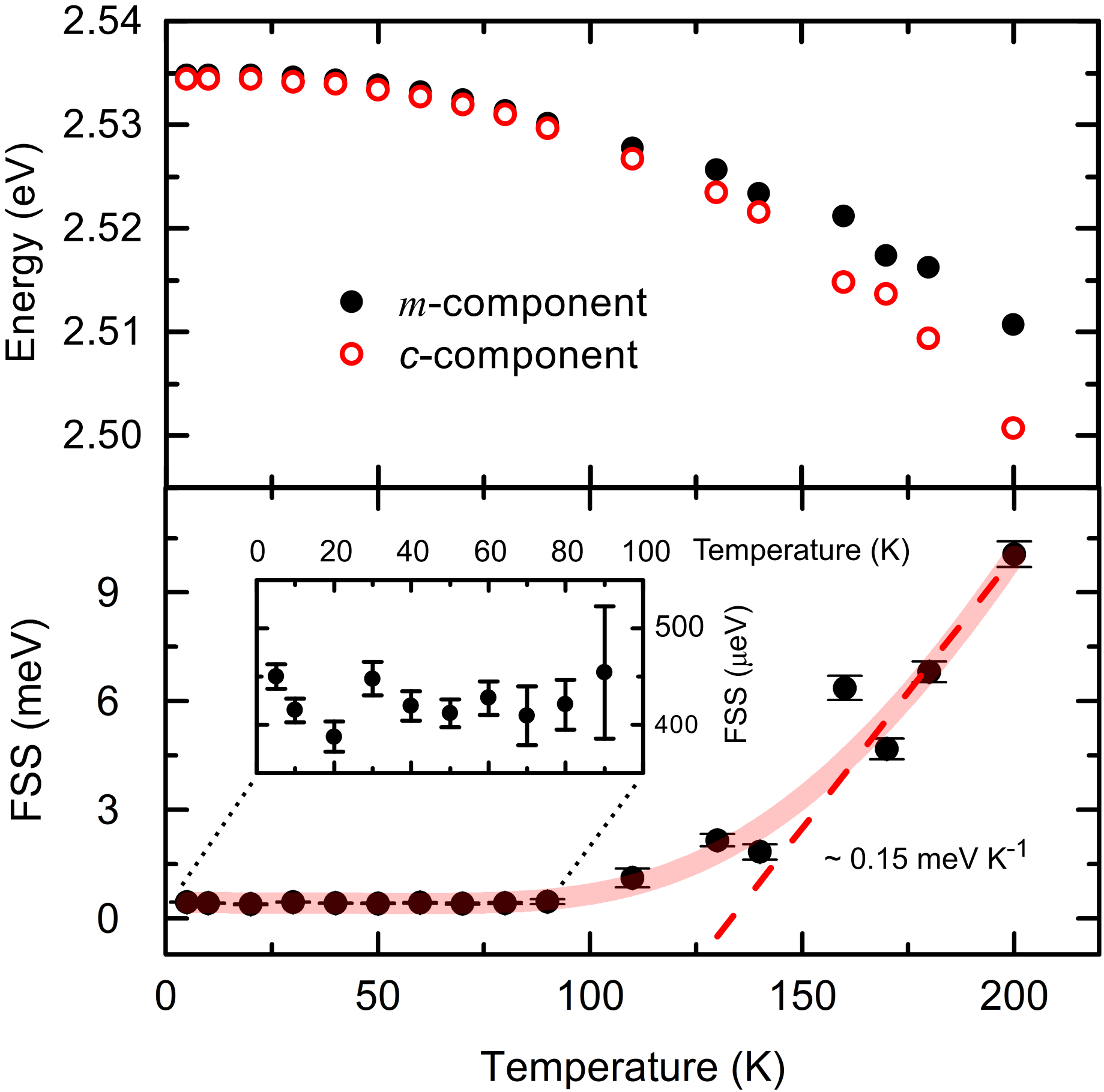
2.54
2.53
2.52
2.51
2.50
Energy (eV)
m-component
c-component
9
6
3
0
FSS (meV)
0
50
100
150
200
Temperature (K)
~ 0.15 meV K-1
0
20
40
60
80
100
Temperature (K)
500
400
FSS (μeV)

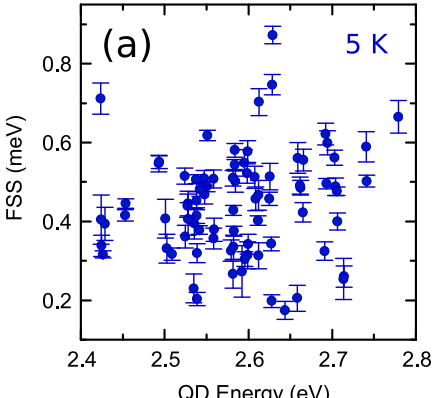
(a)
5 K
FSS (meV)
QD Energy (eV)

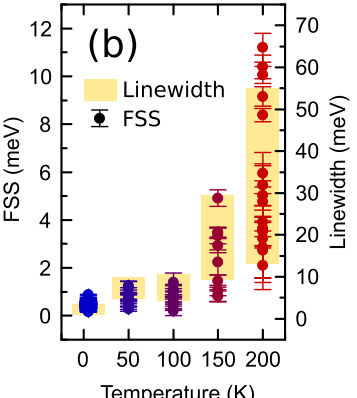
(b)
Linewidth
FSS
FSS (meV)
Linewidth (meV)
Temperature (K)

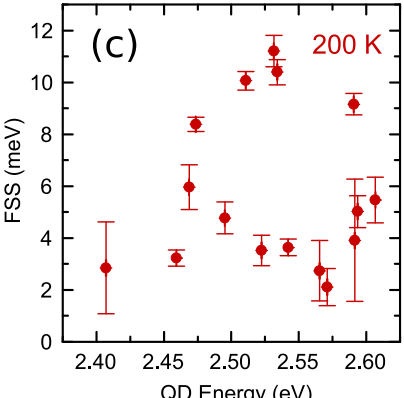
(c)
200 K
FSS (meV)
QD Energy (eV)